Green Synthesis and Characterization of Iron Oxide Nanoparticles for Efficient Removal of Ciprofloxacin from Simulated and Hospital Wastewater

H. I. Adamu*, M. A. Richard, A. Y. Ugya and A. O. Olaniyi

Department of Environmental Management, Kaduna State University, Kaduna - Nigeria
Correspondence Email: habibadamu99@kasu.edu.ng

ABSTRACT

This study explores the synthesis, characterization, and application of iron oxide nanoparticles (IONPs) derived from environmentally friendly sources, specifically mixture of orange peel and rice husk extracts, for the effective removal of ciprofloxacin from simulated and hospital wastewater. The synthesized IONPs were characterized using techniques such as U-Visible spectroscopy, Dynamic light Scattering (DLS), X-ray diffraction (XRD), scanning electron microscopy (SEM), Fourier transform infrared spectroscopy (FTIR) and Brunaur-Emmet-Teller (BET), which confirmed their optical properties, size/its distribution, crystalline structure, morphology, functional groups and surface area. The nanoparticles exhibited a uniform size distribution with Z-average of 94.4 nm and polydispersity index of 0.386, with peaks corresponding to several functional groups, Fe-O bond appearing at $693cm^{-1}$ and a high surface area of 965.55 m²/g, enhancing their adsorption capacity. The efficiency of the IONPs in removing ciprofloxacin was evaluated through batch adsorption experiments with significant percentage reductions observed in both simulated and hospital wastewater. In hospital wastewater samples, the IONPs achieved removal efficiencies of up to 87.1%, indicating their practical applicability in real-world scenarios. Kinetic studies revealed that the adsorption process followed a pseudo-second-order model ($R^2 = 0.9973$), suggesting that the adsorption rate is influenced by the availability of active sites on the nanoparticles. Isotherm studies were conducted using Langmuir, Freundlich, and Temkin models, with the Freundlich model providing the best fit ($R^2 = 0.99536$), indicating heterogeneous adsorption on the nanoparticle surface. The findings highlight the potential of green-synthesized IONPs as an effective and sustainable solution for the removal of pharmaceutical contaminants from wastewater, contributing to environmental remediation efforts and public health protection.

INTRODUCTION

Water pollution stands as a significant environmental challenge, with pharmaceutical contaminants posing severe risks to aquatic ecosystems and human health (Ortúzar *et al.*, 2022). Antibiotics like ciprofloxacin are of special concern due to their widespread usage and persistence in the environment (Khan and Barros, 2023). Hospital wastewater emerges as a major source of these pollutants, highlighting the urgent need for effective treatment methods to mitigate their effects (Eapen *et al.*, 2024). Pharmaceuticals such as antibiotics, analgesics, and hormones are frequently detected in global water bodies, entering the ecosystem through pathways like pharmaceutical manufacturing, improper medication disposal, and human and animal excretion (Papaioannou *et al.*, 2024). Ciprofloxacin, a broad-spectrum antibiotic, is often found in hospital effluents due to its extensive use in treating bacterial infections (Khan &Barros, 2023). Its presence in water bodies can facilitate

the development of antibiotic-resistant bacteria, posing a significant threat to public health.

Nanotechnology provides promising solutions for water treatment, with nanoparticles offering unique properties like high surface area, reactivity, and adaptable surface chemistry (Khan & Barros, 2023). Iron oxide nanoparticles have gained attention for their potential to adsorb various contaminants from water (Cheng *et al.*, 2016). Their magnetic properties allow for easy separation from aqueous solutions, making them ideal candidates for water purification applications (Khan & Barros, 2023).

Traditional nanoparticle synthesis methods often involve toxic chemicals and high energy consumption, raising environmental and safety concerns. Green synthesis offers an eco-friendly and sustainable alternative by utilizing natural resources such as plant extracts, bacteria, and fungi. This study leverages a combination of orange peel and rice husk extracts, agricultural wastes rich in bioactive compounds like phenols, flavonoids, and alkaloids, to synthesize iron oxide

nanoparticles. These compounds serve as reducing and stabilizing agents during nanoparticle synthesis, reducing environmental impact and enhancing nanoparticle biocompatibility (Adamu *et al*., 2023).

The adsorption of ciprofloxacin onto iron oxide nanoparticles involves several mechanisms, including electrostatic interactions, hydrogen bonding, and π-π interactions. The surface charge of the nanoparticles is essential for attracting positively charged ciprofloxacin molecules (Al-Musawi *et al*., 2021). Functional groups on the nanoparticle surface facilitate hydrogen bonding with ciprofloxacin, while π-π interactions between the aromatic rings of ciprofloxacin and the nanoparticle surface further boost adsorption capacity (Khasevani, *et al*., 2023).

Characterizing the synthesized nanoparticles is crucial for understanding their properties and optimizing their performance for adsorption applications. Techniques such as X-ray diffraction (XRD), scanning electron microscopy (SEM), Fourier transform infrared spectroscopy (FTIR), and dynamic light scattering (DLS) analyze the crystalline structure, morphology, functional groups, and particle size distribution of the nanoparticles (Ogbezode *et al*., 2023). These characterization methods offer valuable insights into the synthesis process and the effectiveness of the nanoparticles in adsorbing ciprofloxacin.

Removing pharmaceutical contaminants from water is vital for safeguarding aquatic ecosystems and human health. Iron oxide nanoparticles synthesized using green methods provide a sustainable solution for wastewater treatment (Chaudhari *et al*., 2024). Beyond water purification, these nanoparticles have potential applications in fields like catalysis, drug delivery, and environmental remediation (Priya *et al*., 2021). Developing eco-friendly and efficient adsorption materials supports global efforts to promote sustainable practices and reduce environmental pollution. This study emphasizes the innovative use of green-synthesized iron oxide nanoparticles from the mixture of orange peel and rice husk extracts for the effective adsorption of ciprofloxacin from hospital wastewater.

MATERIALS AND METHODS
Collection of orange peel and rice husk sample
Orange peel and rice husk samples were collected from a fruit market in Bakin Dogo and a local rice milling factory in the Mando area, both within Kaduna Metropolis. These samples were placed in labeled polythene bags and transported to the laboratory. The orange peel was thoroughly washed with distilled water to remove impurities, cut into smaller pieces, and dried in the shade for seven days (Naqvi *et al*., 2021. After drying, the peels were finely ground using a Silver Crest electric blender into a powder, which was then sieved through a 60 mm mesh. The rice husk was

also washed with distilled water and dried under shade and grounded using electric blender. It was using 5mm sieve.

Collection of hospital wastewater
The hospital wastewater samples were collected from three healthcare facilities within Kaduna metropolis. The facilities include two tertiary health facilities labeled as BDSH and YSDH and one primary health facilities labeled PHCBR. These samples were collected using clean 1-liter glass bottles from the discharge point of the health facilities wastewater discharge point. The samples were collected in triplicate and subsequently transported to the laboratory in an ice bath container for analysis.

Preparation of orange peel and rice husk extract mixture
An analytical weighing balance was used to weigh accurately 10 g of the ground orange peel and rice husk powder separately and transferred in to an Erlenmeyer flask, 100 mL deionized water was then added to the flasks and heated mildly at 40°C for 2 hrs. with continuous stirring at 500 rpm/min using a magnetic stirrer. The extract was then filtered using a Buchner filtration and the filtrate stored at 4°C prior to the preparation of the nanoparticles (Jamzad and Kamari Bidkorpeh, 2020; Faisal *et al*., 2021).

Synthesis of the iron oxide nanoparticles
The iron oxide nanoparticles was synthesized methodology described by Thi *et al*., (2020). A 100 mL mixture of orange peel and rice husk extract was measured and transferred into 250 mL conical flasks placed on a magnetic stirrer equipped with a magnetic stirring rode. A 50 mL Fe^{2+} and Fe^{3+} salt solution (1:2 molar ratio) were added gradually while stirring. The pH was adjusted to 11 using 1.0 M NaOH, and the solution was stirred for an hour, then cooled. The mixture was centrifuged at 5000 rpm for 10 minutes to separate nanoparticles, which were filtered, washed with deionized water and ethanol, dried at 130°C, and stored. Nanoparticle formation was confirmed by colour change and UV-Vis spectroscopy.

Characterization of the synthesized iron oxide nanoparticles
The synthesized iron oxide nanoparticles were characterised using the Fourier Transformed infra-red spectroscopy (Shimadzu Fourier Transform Infrared Spectrophotometer-FTIR 8400 S) at the Multi-user laboratory of Ahmadu Bello University Zaria covering 4000-400cm^{-1} for it functional groups, its optical properties using UV-visible spectroscopy (T70 PG Instruments UV-Visible absorption spectrophotometers, ranging from 200 to 800 nm), the surface morphology and elemental composition using Scanning electron microscopy coupled with Energy-Dispersive X-ray

analysis (Scanning Electron Microscope model JOEL JSM 7600F) located at National Steel Raw Material and Exploration Agency in Kaduna. The surface area of the iron oxide nanoparticles was studied using Brunneur-Emmet-Teller (BET) 9 JW-DA: 76502057en China equipment) respectively while the crystal structure and size was determined using Dynamic light scattering technique (Malvern Panalytical Zetasizer with multi-angle light scattering Nano ZS90 and Rigaku MiniFlex 6G XRD machine) at Step B laboratory located in

Federal University of Technology Minna and National Steel Research and Exploration Agency Kaduna respectively.

Batch adsorption studies
The adsorption of ciprofloxacin was studied using experimental technique as outline by Ahmadpour *et al*., (2019) using the simulated wastewater. The optimal parameters were determined by varying the parameters as presented on the Table 1.

Table 1: Adsorption Parameters

Parameters	Variations
Adsorbent dose	20, 40, 60, 80,100, 100 mg
adsorbate concentration	2, 4, 6, 8, 10 mg/l
Time	5, 10, 15, 20, 25, 30, 35, 40 min
pH	3, 5, 7, 9, 11
Temperature	27, 32, 37, 42°C

The point of zero charge was determined by the method described by Bakatula *et al*. (2018). The quantity of ciprofloxacin adsorbed under the different experimental condition was calculated using the equations 1 and 2.

$$qe = \frac{(Co-Ce)V}{W} \qquad (1)$$

$$\% \, Removal = \frac{Co-Ce}{Co} * 100 \qquad (2)$$

Here, (q_e) represents the adsorption amount of ciprofloxacin (mg/g) in the solid at equilibrium; (C_o) and (C_e) are the initial and equilibrium concentrations of the pharmaceutical (mg/L), respectively; (V) is the volume (ml) of the aqueous solution, and (W) is the mass (g) of the adsorbent used in the experiments.

Determination of the concentrations of ciprofloxacin from hospital wastewater and its removal with the synthesized IONPs
The concentration of ciprofloxacin in the hospital wastewater was determined using microplate reader. A 250 µL of the sample was accurately measured using a micropipette and transferred to a clean microplate in triplicate and

analyzed at a wavelength of 280 nm for the ciprofloxacin respectively. The concentration of ciprofloxacin was calculated from a calibration curve.
The adsorption experiments were conducted using the procedure outlined for the batch adsorption experiment using the optimum adsorption parameters obtained.

Kinetic Studies
Kinetic studies are crucial for understanding ciprofloxacin adsorption onto adsorbents like iron oxide nanoparticles. They assess removal rates and provide process insights using key models. The Pseudo-First-Order Model relates adsorption rate to available sites, while the Pseudo-Second-Order Model emphasizes site availability over adsorbate concentration, fitting ciprofloxacin data better. The Intraparticle Diffusion Model considers pore diffusion as a limiting factor, and the Elovich Model describes chemisorption kinetics, useful for heterogeneous surfaces with varying activation energies (de Oliveira Carvalho *et al*., 2018). The linear equation of the kinetic models are presented on Table 2.

Table 2: Linear Kinetic models (de Oliveira Carvalho *et al*., 2018)

Kinetic model	Linear equations
Pseudo 1st order	$\ln(q_e - q_t) = lnq_e - k_i t$
Pseudo 2nd order	$\frac{t}{qt} = \frac{1}{K_2 q_e^2} + \frac{1}{q_e}$
Interparticle diffusion	$q_t = k_p t^{1/2} + C$
Elovich	$q_t = \frac{1}{\beta}\ln(\alpha\beta) + \frac{1}{\beta} lnt$

Where (q_e) and (q_t) (both in mg/g) represent the amount of adsorbate adsorbed per unit mass of adsorbent at equilibrium and at time "t," respectively. The adsorption rate constant (K_1) for pharmaceutical sorption will be determined from the slope of the linear plot of ln (q_e- q) vs time (t) for the first order rate law.

Also, (q_e) and (q_t) (both in mg/g) denote the amount of ciprofloxacin adsorbed per unit mass of adsorbent at equilibrium and at time "t," respectively. The value of (k') can be derived from the slope of the plot of (t/q_t) against (t), where (t) is the time (in seconds or minutes) and (q_t) is the concentration of the limiting reactant or the amount of adsorbate per unit mass of adsorbent at time (t) (in mol/L or mg/g) for the second order rate law.

For the interparticle diffusion, (q_t) represents the amount of adsorbate per unit mass of adsorbent at time (t) (mg/g), (k_p) is the interparticle diffusion rate constant (mg/g min$^{1/2}$), (t) is the time (minutes), and (C) is the intercept (mg/g), which indicates the boundary layer effect. The value of (k_p) indicates the rate of interparticle diffusion. The higher the value of (k_p), the faster the interparticle diffusion. The value of C indicates the boundary layer effect. A larger value of (C) signifies a stronger boundary layer effect (Vijaykumar *et al*., 2016).

Lastly, the Elovich kinetic model present, (q_t) as the amount of adsorbate per unit mass of adsorbent at time (t) (mg/g), (α) represents the initial adsorption rate (mg/g min), (β) is the desorption constant (g/mg), and (t) is the time (minutes). The value of (α) reflects the initial speed of the adsorption process. The higher the value of (α), the faster the adsorption. A greater value of (α) signifies a quicker adsorption process. The value of (α) reflects the level of surface heterogeneity, with a higher (β) indicating a more heterogeneous surface.

Adsorption Isotherm

To elucidate the adsorption mechanism and determine key adsorption parameters, the experimental data will be analyzed using three prominent isotherm models: Langmuir, Freundlich, and Temkin. The Langmuir isotherm equation, which assumes monolayer adsorption on a homogeneous surface, will be employed to investigate the adsorption process and estimate relevant parameters.

The linear form of the Langmuir isotherm is as shown in Equation (3), to identify the adsorption parameters (Ayawei *et al*., 2017).

$$\frac{1}{q_e} = \frac{1}{K_L q_{maz}} \cdot \frac{1}{C_e} + \frac{1}{q_{max}} \qquad (3)$$

In this context, K_L is the Langmuir constant (L/mg), indicating adsorption energy, q_{max} is the maximum adsorption capacity (mg/g), representing the highest amount of pharmaceutical adsorbed per

gram at equilibrium, and C_e is the equilibrium concentration (mg/L) of the adsorbate. A linear plot of 1/qe versus 1/Ce allows extraction of q_{max} and K_L from the slope and intercept. The fit's accuracy is assessed by the coefficient of determination (R^2), with values near 1 indicating a strong fit to the Langmuir model. The separation factor R_L, a dimensionless constant, predicts adsorption efficiency and evaluates feasibility.

This factor can be calculated using the following equation, enabling the evaluation of the adsorption process's feasibility and potential performance.

$$R_L = \frac{1}{1 + K_L C_0} \qquad (4)$$

In this context, K_L represents the Langmuir constant (mg/L), and Co denotes the initial concentration of the adsorbate (mg/L). The dimensionless separation factor (R_L) indicates the adsorption feasibility: unfavorable adsorption occurs when $R_L > 1$, linear adsorption when $R_L = 1$, favorable adsorption when $0 < R_L < 1$, and irreversible adsorption when $R_L = 0$.

The Freundlich isotherm (equation 5), indicating that adsorption takes place on a heterogeneous surface (Alfonso *et al*., 2016), is presented as follows.

$$log q_e = \log K_F + \frac{1}{n} log C_e \qquad (5)$$

In this context, K_F and n are isotherm constants indicating adsorption capacity and intensity, while 1/n reflects adsorption strength. A linear plot of log (q_e) versus log (C_e) reveals a slope of 1/n and an intercept of ln (K_F), from which the Freundlich constants can be determined. The goodness of fit is measured by the coefficient of determination (R^2), with values close to 1 indicating a more accurate data representation.

The Temkin isotherm model accounts for indirect adsorbate interactions, assuming that the heat of adsorption decreases linearly as surface coverage increases. The linear form of Temkin isotherm model described by Ayawei *et al*., (2017) is given by equation 6.

$$\ln (q_e) = \ln (a) + \frac{RT}{b} \ln (C_e) \qquad (6)$$

Plotting ln (q_e) against ln (C_e) creates a straight line with a slope of RT/b and an intercept of ln(a), from which 'a' and 'b' can be determined. The fit quality is evaluated using the coefficient of determination (R^2), where values near 1 signify a better fit.

RESULTS AND DISCUSSION
Characterization of the synthesized iron oxide nanoparticles
FTIR analysis: The spectral analysis of the synthesized iron oxide nanoparticles reveals several

key peaks that provide insights into their composition and the role of plant extracts in their stabilization. At 693.28 cm⁻¹, the peak is typically linked to the Fe-O stretching vibration, a clear indicator of the presence of iron oxide nanoparticles (Sithara *et al.*, 2024). This foundational vibration underscores the successful synthesis of the nanoparticles, confirming their core structure.

Moving to the mid-infrared region, the peak at 1133.11 cm⁻¹ likely corresponds to C-O stretching vibrations. This feature is attributed to organic compounds originating from the plant extracts used during synthesis, such as orange peel and rice husk extracts (Rojo *et al.*, 2024). These compounds are integral to the nanoparticle formation process, contributing to the unique chemical environment around the nanoparticles.

The peak at 2139.49 cm⁻¹, although less common in typical iron oxide spectra, suggests the presence of certain organic functional groups or impurities. These might have been derived from the organic matrix provided by the plant extracts, indicating a potential complexity added by these natural substances during synthesis (Bashir *et al.*, 2020).

In the higher frequency range, the peaks at 3183.14 cm⁻¹ and 3384.42 cm⁻¹ are both indicative of O-H stretching vibrations. These peaks suggest the presence of hydroxyl groups, which could originate from residual water or the plant extracts themselves (Bashir *et al.*, 2020). The presence of these groups is significant as they play a crucial role in capping and stabilizing the nanoparticles, ensuring their stability and dispersibility in various environments (Demirezen *et al.*, 2019). The spectral data not only confirmed the successful synthesis of iron oxide nanoparticles but also highlights the important role of plant extracts in their stabilization. The presence of both O-H and C-O stretching vibrations verifies the capping effect of the organic compounds, which aids in maintaining the structural integrity and functionality of the nanoparticles (Elkhateeb *et al.*, 2024).

UV-Visible spectroscopic analysis: The UV-Visible spectroscopic analysis of iron oxide nanoparticles, synthesized using orange peel and rice husk extracts, reveals an intriguing absorbance peak at 270 nm as shown on Fig 1. This peak is primarily associated with electronic transitions occurring within the nanoparticles, specifically the charge transfer transitions between Fe^{3+} and O^{2-} ions. These transitions are fundamental in understanding the optical properties of the nanoparticles, as they signify the interactions occurring at the molecular level within the iron oxide structure (Varghese *et al.*, 2023)

Furthermore, the presence of organic compounds from the orange peel and rice husk extracts plays a crucial role in influencing these optical properties. These plant extracts not only contribute to the absorbance characteristics observed but also assist in the successful capping and stabilization of the nanoparticles. This capping effect is vital as it enhances the stability and dispersibility of the nanoparticles, ensuring their effectiveness and functionality in various applications (Vikram *et al.*, 2016).
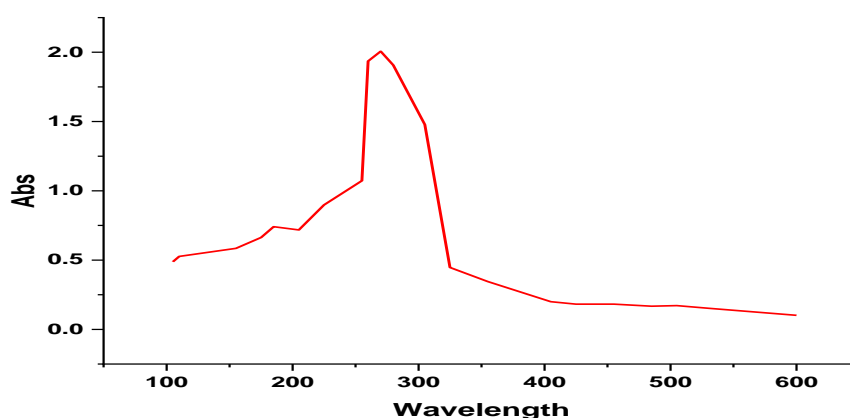

Fig 1: UV-Visible spectra of the iron oxide nanoparticles

Dynamic light scattering (DLS) analysis: The Z-average, or intensity-weighted mean hydrodynamic diameter, provides insight into the average size of nanoparticles in the sample. With a Z-average of 94.40 nm, the iron oxide nanoparticles are relatively small, making them well-suited for applications like environmental remediation and wastewater treatment. This smaller size confers a larger surface area-to-volume ratio, enhancing their reactivity and adsorption capacity for environmental contaminants (Ogbezode *et al.*, 2023; Savari & Jabali, 2023).

The Polydispersity Index (PDI) characterizes the distribution of particle sizes within the IONPs. A moderate PDI value of 0.386 indicates a relatively narrow size distribution (Fig 2), which is desirable for consistent performance in various applications (Ysain *et al.*, 2023). For context, a PDI below 0.1 suggests a very uniform size distribution, while values above 0.5 indicate a broad distribution. The PDI value suggests a balanced size distribution, striking a favorable balance between uniformity and diversity in nanoparticle size (Savari & Jabali, 2023).
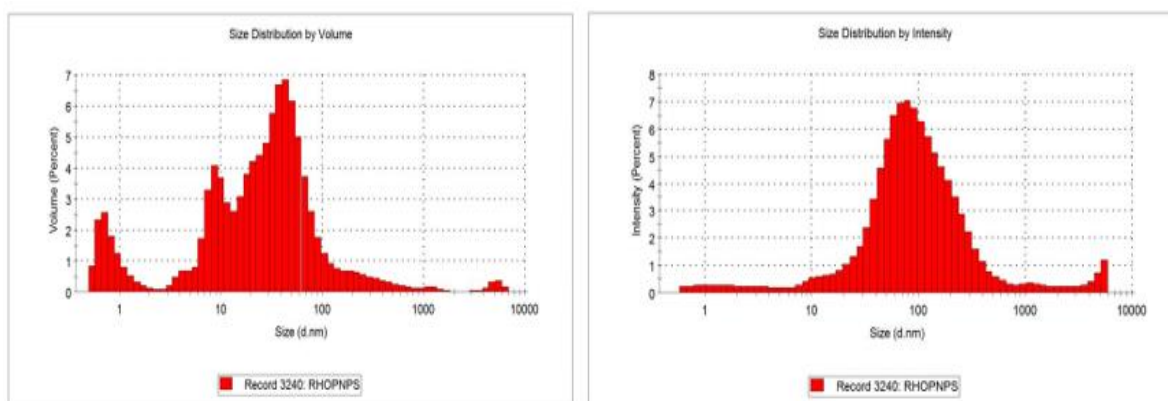

Fig 2: Size distribution by volume and intensity

Scanning Electron microscopy/Energy Dispersive Electron Spectroscopy: The SEM micrograph of iron oxide nanoparticles synthesized from a mixture of rice husk and orange peel in the ratio of 1:1 calcined at 450°C for two hours as presented in Plate 1 showed that the surface morphology of the particles is rough with roughly spherical shape, this is further confirmed from the PDI of 0.386 reported for the DLS analysis of the nanoparticles. Hence, it can be deduced that the combination of the plant extract result in the formation of nanoparticles with reduced aggregation due the capping abilities of polyphenols in the mixture of the plant extracts (Aryal *et al.*, 2019). The size of the nanoparticles determined by analysis of the micrograph using imageJ software was between the ranges of 12-41 nm with an average of 27.64 nm which far less than the 94 nm reported from the DLS analysis. Balamurugan *et al.* (2014) reported similar SEM

result for iron oxide nanoparticles synthesized from Eucalyptus globulus plant extract.

The synthesis of iron oxide nanoparticles was also confirmed through the significant iron content, which constitutes 76.85% of the composition, with a binding energy of 5.0 keV that is characteristic of iron as confirmed using the energy dispersive spectroscopy as shown on Fig 3. This indicates the presence of Fe^{3+} ions in the nanoparticle structure. Additionally, the oxygen content of 22.04% at 0.5 keV is in line with the formation of iron oxide, either Fe_2O_3 or Fe_3O_4, suggesting that the iron is oxidized to form the desired nanoparticles. Furthermore, a small carbon content of 2.20% at 1.0 keV, likely originating from organic compounds in the orange peel and rice husk extracts, acts as capping agents. These organic compounds play a crucial role in stabilizing the nanoparticles and preventing their aggregation.
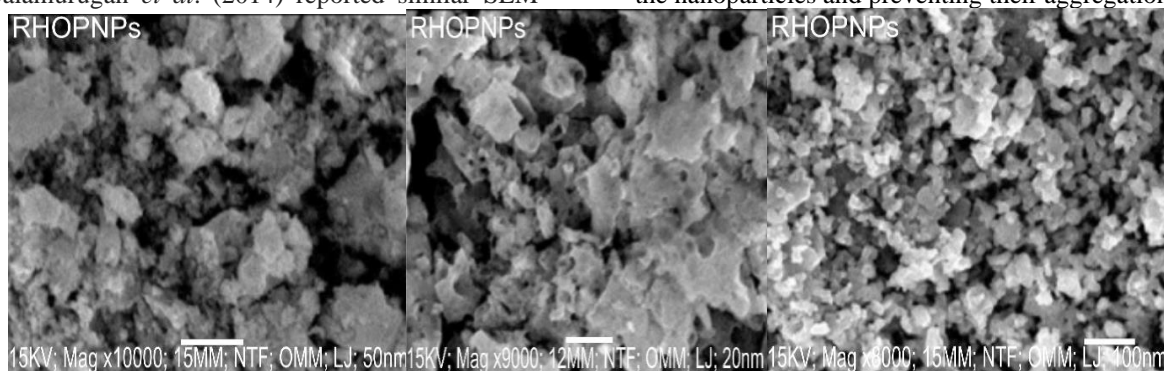
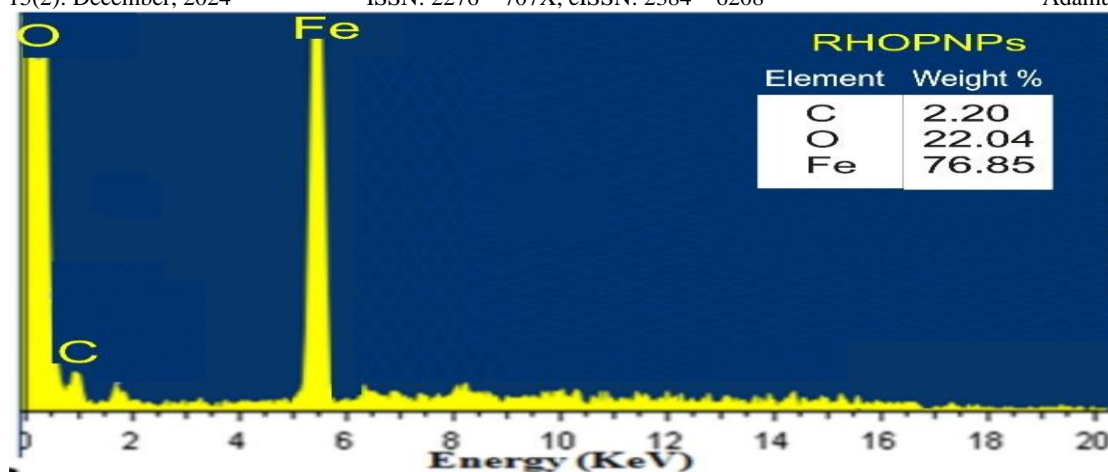**Plate 1: SEM micrograph of the iron oxide nanoparticles at magnification of 10,000, 9000 and 8000**

Fig. 3: EDX spectra of the iron oxide nanoparticles

X-ray diffraction spectroscopy: Analysis of the XRD result for iron oxide nanoparticles synthesized from the orange peel and rice husk extract mixture (Fig. 4) reveals a specific diffraction peak at $2\theta = 35.74°$ with Miller indices (HKL) of 113. This indicates a cubic-centered crystal system of magnetite (Fe_3O_4), confirming the material's crystalline nature (Sing *et al.*, 2021). The space group is identified as FD-3M (space group number 227), describing the symmetry elements and atomic arrangements within the crystal lattice. This information helps determine the crystal's internal structure, symmetry operations, and unit cell dimensions, indicating cubic symmetry.

The ICSD collection code 158746 (reference code 98-010-9828) closely matches the observed XRD pattern, facilitating identification of the material's crystal structure and reference database entry (Mourdikoudis *et al.*, 2018). Using the Debye-Scherrer equation, the crystal size is calculated as 134.18 nm, considering the most intense peak ($2\theta = 35.74°$) and full width at half maxima (0.065). Notably, this value is higher than the Z-average (76.24 nm) from DLS analysis and the SEM-derived size range (12-41 nm, average 27.64 nm).

Similar XRD patterns for iron oxide nanoparticles synthesized from the orange peel and rice husk extract mixture indicate crystallinity, with intense diffraction peaks at $2\theta = 35.74°$. However, broad peaks suggest the presence of amorphous particles (Stan *et al.*, 2017; Razack *et al.*, 2020).
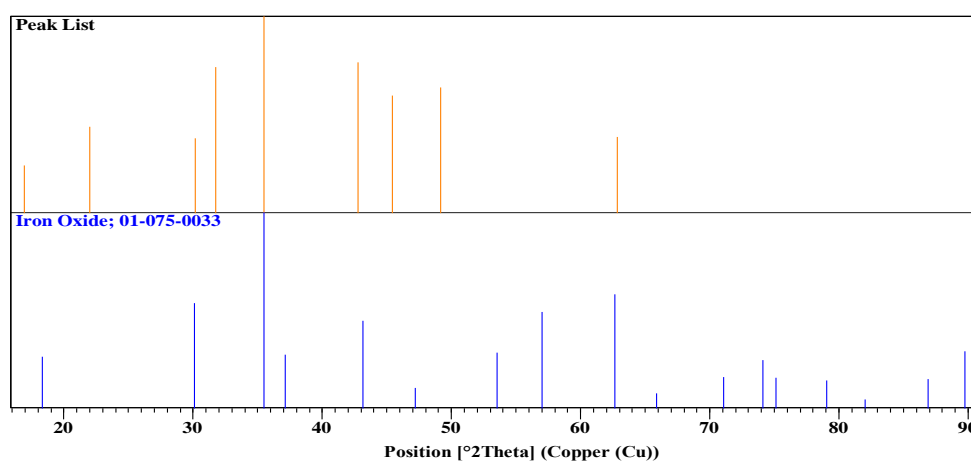

Fig 4: XRD spectra of the iron oxide nanoparticles

Brunauer–Emmett–Teller (BET): The nanoparticles exhibit a remarkably high BET surface area of 965.55 m²/g, indicating an abundance of surface available for adsorption. This exceptional surface area is particularly beneficial for applications such as catalysis, adsorption, and environmental remediation, as it provides a vast number of active sites for interactions with other molecules (Lavín Flores *et al.*, 2024).

In contrast, the Langmuir surface area of 66.52 m²/g is lower, suggesting that the surface may not be entirely homogeneous or that multiple layers of adsorption are occurring. Nevertheless, this value still indicates a significant surface area, highlighting the nanoparticles' potential for adsorption and interaction. The pore volume of 0.62556 cm³/g reveals the total volume of pores within the nanoparticles, indicating a porous structure that enhances their ability to adsorb and

interact with various substances. This is particularly advantageous in applications like drug delivery and pollutant removal, where a high pore volume can improve efficiency (Hernández-Hernández *et al.*, 2020).

The adsorption isotherm is characterized as Type II, typical of non-porous or macroporous materials, indicating multilayer adsorption. The condensation range of 0.05-0.9 suggests a variety of pore sizes, beneficial for applications requiring different adsorption capacities.

The implications of these findings are significant. The high surface area and pore volume make the nanoparticles highly effective for adsorption applications, suitable for environmental remediation and catalysis. The porous structure and Type II isotherm suggest stability and efficiency in intended applications, including drug delivery and pollutant removal (Dhal *et al.*, 2020).

Batch Adsorption Studies of Ciprofloxacin
Effect of adsorbent dosage and contact time
The results of the effect of adsorbent dose and contact time shows that the adsorption efficiency varies with different adsorbent doses and contact times (Fig 5).

The effect of adsorbent dose was examined at five different levels: 20 mg, 40 mg, 60 mg, 80 mg, and 100 mg. The results indicate that the highest adsorption efficiency was achieved with 100 mg of adsorbent, reaching 90.36% at 40 minutes. This suggests that increasing the

adsorbent dose enhances the removal efficiency of ciprofloxacin (Azizi, 2021).

The effect of contact time was also studied, revealing three distinct phases. The initial phase (0-10 minutes) showed rapid adsorption across all doses, indicating a high availability of active sites on the nanoparticles. The middle phase (10-25 minutes) saw ongoing adsorption processes with some fluctuations, while the final phase (25-40 minutes) showed stabilization or slight decreases in adsorption efficiency, suggesting that equilibrium was being approached.

The optimal adsorbent dose was found to be 100 mg, which achieved the highest adsorption efficiency. The rapid initial adsorption indicates that the nanoparticles have a high affinity for ciprofloxacin, making them effective for quick removal (Al-Musawi *et al.*, 2021). The stabilization of adsorption efficiency in the final phase suggests that equilibrium is being reached, where the rate of adsorption equals the rate of desorption.

The results demonstrate that the iron oxide nanoparticles synthesized using orange peel and rice husk extracts are highly effective for the adsorption of ciprofloxacin from wastewater. The adsorption efficiency is influenced by both the adsorbent dose and contact time, with higher doses and longer contact times generally leading to higher removal efficiencies (Al-Musawi *et al.*, 2021). These findings highlight the potential of these nanoparticles for environmental remediation applications, particularly in the removal of pharmaceutical contaminants from wastewater.
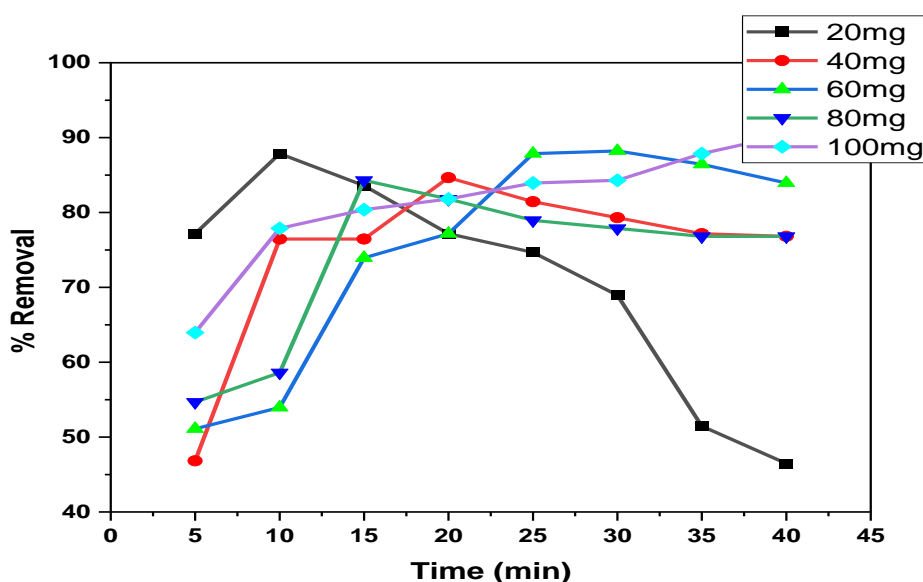
Fig. 5: Effect of adsorbent dosage and contact time on the adsorption of ciprofloxacin using the IONPs
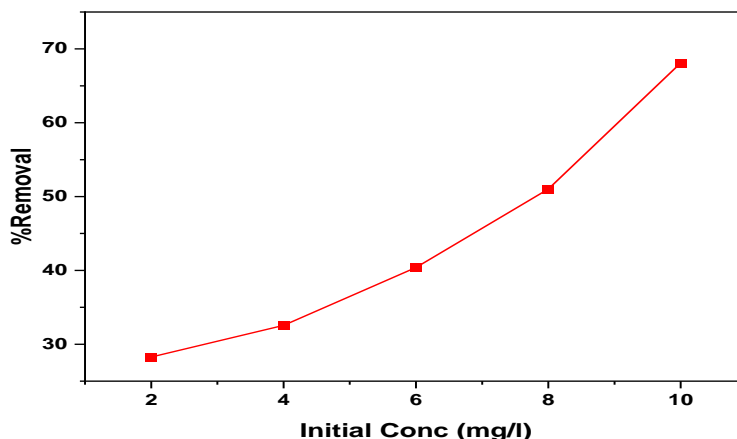
Effect of Initial adsorbate concentration
The results of the effect of initial adsorbate concentration on the adsorption of ciprofloxacin showed a positive correlation between initial concentration and percentage removal, with removal efficiency increasing from

28.27% at 2 mg/L to 68.09% at 10 mg/L (Fig. 6). This trend suggests that higher concentrations enhance mass transfer, allowing ciprofloxacin molecules to reach their binding sites more effectively (Xing *et al.*, 2015). This is consistent with findings from a similar study on

organophosphate pesticide removal (Mehta *et al*., 2022). However, removal efficiency may not increase indefinitely with concentration, as factors

like pH, temperature, adsorbent concentration, and incubation time can also impact adsorption (Adegoke *et al*., 2023).

Fig 6: Effect of initial concentration on the adsorption of ciprofloxacin using the IONPs
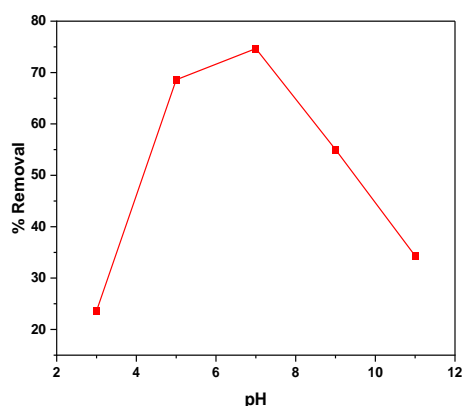
Effect of pH

The results show a significant impact of pH on removal efficiency (Fig 7). At pH 3, the removal efficiency was 23.63%, increasing to 68.59% at pH 5, and peaking at 74.66% at pH 7. However, at pH 9 and pH 11, the removal efficiency decreased to 55.03% and 34.33%, respectively. This trend suggests that near-neutral conditions are most favorable for ciprofloxacin removal.

The increase in removal efficiency from acidic to neutral pH can be attributed to changes in the surface charge of the nanoparticles and the ionization state of ciprofloxacin (Ibraheem *et al*., 2022). Below the point of zero charge (pH 6) as shown on Fig 8, the nanoparticles are positively charged, leading to repulsion between the

nanoparticles and ciprofloxacin molecules (Ibraheem *et al*., 2022). Near-neutral pH conditions may favor the optimal ionization state for adsorption. The decrease in removal efficiency beyond pH 7 could be due to changes in the surface charge and ionization state, affecting the adsorption process (Oliveira *et al*., 2024).

The high removal efficiency at near-neutral pH has significant implications for practical applications. These conditions are ideal for wastewater treatment, highlighting the potential of these green-synthesized nanoparticles for environmental remediation. Optimizing pH levels can enhance the effectiveness of ciprofloxacin removal, contributing to safer water management practices (Sassa-Deepaeng *et al*., 2024).
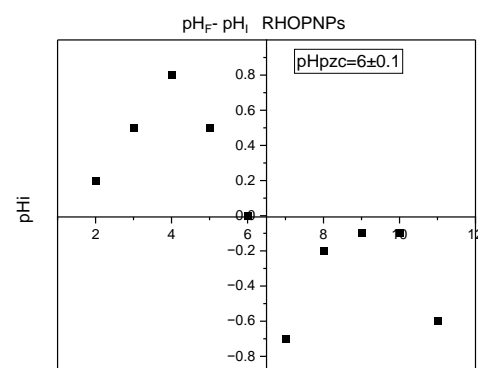

Fig 7: Effect of pH on the adsorption of ciprofloxacin using the IONPs

Fig 8: The pH$_{pzc}$ of the IONPs

Effect of temperature

The removal of ciprofloxacin from water using iron oxide nanoparticles synthesized from a mixture of orange peel and rice husk was investigated at various temperatures as shown of

Fig 9. The results show a positive correlation between temperature and percentage removal.

At 300 K, the removal efficiency was 67.52%, increasing to 78.27% at 305 K, 84.27% at 310 K, 88.37% at 315 K, and peaking at 93.43% at

320 K. This trend suggests that higher temperatures enhance the adsorption process, possibly due to increased kinetic energy and more effective collisions between ciprofloxacin molecules and the nanoparticles.

The increased kinetic energy at higher temperatures leads to more frequent and effective collisions, while also enhancing the diffusion rate of ciprofloxacin molecules towards the adsorption sites. This results in improved overall adsorption efficiency (Gor *et al*., 2020). Leveraging temperature variations can optimize the adsorption process, and understanding the effect of temperature on adsorption efficiency can inform the design of more effective water treatment systems using green-synthesized nanoparticles (Al-Musawi *et al*., 2021).
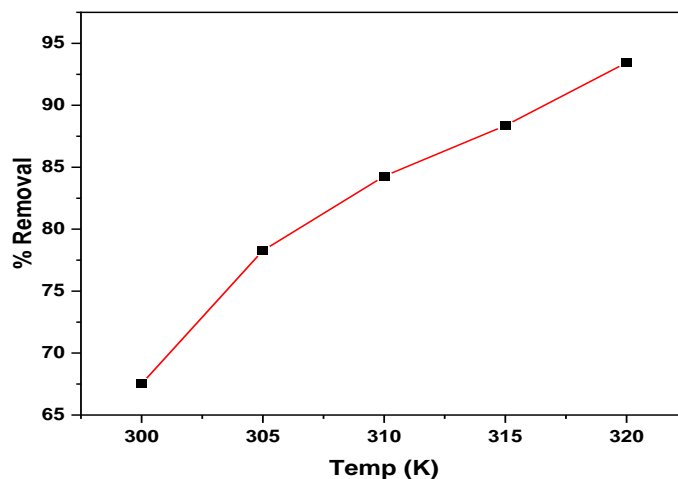
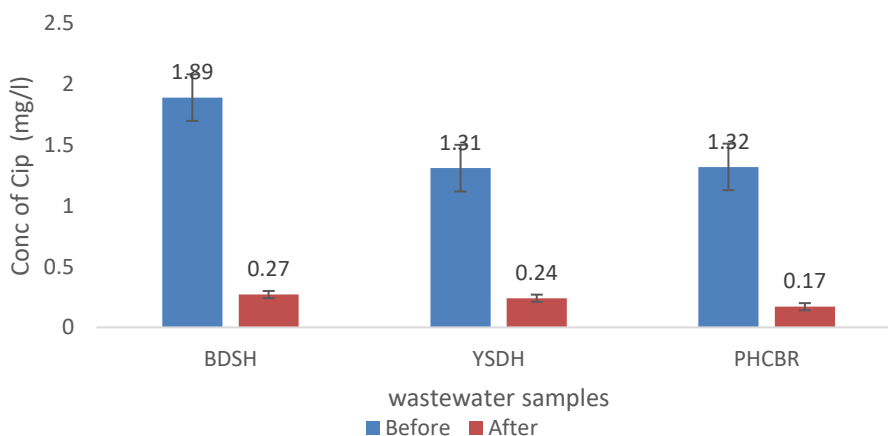**Fig 9: The effect of temperature on the adsorption of ciprofloxacin using the IONPs**

Determination and removal of ciprofloxacin in hospital wastewater

The efficacy of synthesized iron oxide nanoparticles (IONPs) in removing ciprofloxacin from hospital wastewater was evaluated using three samples: BDSH, YSDH, and PHCBR. Initially, the concentrations of ciprofloxacin were 1.89, 1.31, and 1.32 mg/L, respectively. Following treatment with IONPs, the concentrations significantly decreased to 0.27, 0.24, and 0.17 mg/L, representing reductions of 85.70, 81.70, and 87.1%, respectively as presented on Fig 10.

These remarkable reductions underscore the high efficiency of IONPs as adsorbents for ciprofloxacin, demonstrating their potential for environmental remediation (Mutia *et al*., 2022) The significant decrease in ciprofloxacin concentrations highlights the ability of IONPs to mitigate pharmaceutical contaminants in hospital wastewater, which is crucial for reducing the environmental impact of these pollutants. Pharmaceutical pollutants can contribute to antibiotic resistance and harm aquatic ecosystems (Dhal *et al*., 2020; Shah *et al*., 2022).

Notably, the green synthesis method utilizing orange peel and rice husk extracts provides an eco-friendly approach to nanoparticle synthesis, enhancing their practical applicability in real-world scenarios. This sustainable approach aligns with the growing need for environmentally responsible solutions (Aswathi *et al*., 2023).

Fig 10: Determination and removal of ciprofloxacin in hospital wastewater

Adsorption Isotherm Studies

The adsorption isotherm results for ciprofloxacin using iron oxide nanoparticles synthesized from a mixture of orange peel and rice husk extracts were analyzed using different isotherm models as presented on Table 3. The Langmuir isotherm model, which assumes monolayer adsorption on a homogeneous surface, showed a good fit with an R^2 value of 0.98954. This suggests that the adsorption of ciprofloxacin onto the nanoparticles follows the Langmuir model well, with a maximum adsorption capacity (q_m) of 5.17464 mg/g and a favorable separation factor (R_L) value of 0.01915.

In addition, the Freundlich isotherm model, which describes adsorption on heterogeneous surfaces, showed an excellent fit with an R^2 value of 0.99536. This indicates that the adsorption process is also well described by the Freundlich model, with a value of n (1.58548) greater than 1, indicating favorable adsorption. The Freundlich constant (K_F) of 2.77734 reflects the adsorption capacity and intensity.

Furthermore, the Temkin isotherm model, which considers indirect adsorbate/adsorbate interactions, showed a very good fit with an R^2 value of 0.99538. This suggests that the Temkin model also describes the adsorption process well, with a constant β (3930.14 J/mol) related to the heat of adsorption, indicating significant energy interactions.

The high adsorption capacity indicated by the Langmuir model suggests that the nanoparticles are effective for removing ciprofloxacin from wastewater. The Freundlich model's good fit suggests surface heterogeneity, typical for materials synthesized using natural extracts. The Temkin model's fit indicates significant energy interactions, important for understanding the adsorption mechanism (Al-Musawi *et al*., 2021; Hussain *et al*., 2023). Hence, the good fits of the Langmuir, Freundlich, and Temkin models suggest a complex adsorption process involving monolayer adsorption, surface heterogeneity, and energy interactions.

Table 3: The adsorption isotherms parameters for the adsorption of ciprofloxacin

Isotherm	Parameters	Values
Langmuir	q_m(mg/g)	5.17464
	K_L(l/mg)	1.21962
	R_L (mg/l)	0.01915
	R^2	0.98954
Freundlich	1/n	0.63072
	n	1.58548
	K_F(mg/g)(l/mg)$^{1/n}$	2.77734
	R^2	0.99536
Temkin	RT/b	0.63072
	ln(a)	1.0215
	a(L/g)	2..7773
	B(J/mol)	3930.14
	R^2	0.99538

Kinetic Studies

The adsorption of ciprofloxacin using iron oxide nanoparticles synthesized from a mixture of orange peel and rice husk extracts were analyzed using various kinetic models is presented on Table 4. The pseudo-first order model showed a poor fit, with a low R^2 value of 0.87204 and a negative k_1 value, indicating an unfavorable adsorption rate (Shah *et al*., 2022). In contrast, the pseudo-second order model provided an excellent fit, with a high R^2 value of 0.99737, suggesting chemisorption as the dominant mechanism. This model revealed a higher adsorption capacity, with a qe value of 2.82382 mg/g, indicating the nanoparticles' effectiveness in removing ciprofloxacin (Al-Musawi *et al*., 2021).

The interparticle diffusion model showed a moderate fit, with an R^2 value of 0.86320,

indicating that while diffusion plays a role, it is not the sole rate-controlling step. The Elovich model, which describes chemisorption on heterogeneous surfaces, showed a good fit, with an R^2 value of 0.92823. This model revealed a high initial adsorption rate and suggested surface heterogeneity, typical for materials synthesized using natural extracts (López-Luna *et al*., 2019).

The implications of these findings are significant. The dominance of chemisorption suggests a strong interaction between the nanoparticles and ciprofloxacin, leading to effective removal. The high adsorption capacity and surface heterogeneity of the nanoparticles make them suitable for removing pharmaceutical contaminants from wastewater (Shah *et al*., 2022).

Table 4: Kinetic models for the adsorption of Ciprofloxacin using the synthesized IONPs

Kinetic models	Parameters	Values
Pseudo 1st order	q_e(mg/g)	1.34189
	k_1 (min^{-1})	-0.00047
	R^2	0.87204
Pseudo 2nd order	q_e(mg/g)	2.82382
	q_e^2	7.97396
	k_2(g/mgmin)	0.13671
	R^2	0.99737
Interparticle diffusion	k_p(mg/gmin$^{1/n}$)	0.16171
	C (mg/g)	1.70221
	R^2	0.86320
Elovich	α(mg//gmin)	26.8069
	β (g/mg)	3.0021
	R^2	0.92823

CONCLUSION

In conclusion, the synthesis and characterization of iron oxide nanoparticles using environmentally friendly methods, specifically through the combination of orange peel and rice husk extracts, demonstrate a promising approach to addressing the critical issue of water pollution caused by pharmaceutical contaminants such as ciprofloxacin. The green synthesis method not only minimizes environmental impact but also enhances the stability and efficacy of the nanoparticles due to the natural capping agents present in the plant extracts. The characterization results confirm the successful formation of nanoparticles with desirable properties, including reduced agglomeration and optimal size for application in water treatment processes. The potential of these biogenic iron oxide nanoparticles in degrading and adsorbing pharmaceutical pollutants highlights their role as a sustainable solution in environmental remediation. Future research should focus on optimizing the synthesis process, exploring the full range of applications for these nanoparticles, and conducting extensive field studies to evaluate their effectiveness in real-world scenarios.

ACKNOWLEDGEMENT

REFERENCE

Adamu, H. I., Faruruwa, M. D., Adeyemi, M. M., Tomori, W. B., & Akorede, A. O. (2024): Plant Synthesized Iron Oxide Nanoparticles for Removal of Emerging Contaminant. *Chemistry Africa*, *7*(3), 1173-1186.

Adegoke, K. A., Akinnawo, S. O., Adebusuyi, T. A., Ajala, O. A., Adegoke, R. O., Maxakato, N. W., and Bello, O. S. (2023): Modified biomass adsorbents for removal of organic pollutants: a review of batch and optimization studies. *International Journal of Environmental Science and Technology*, 1-30.

Ahmadpour, A., Fallah, S., and Towfighi, J. (2019): Synthesis and characterization of nanostructured NiO/Al$_2$O$_3$ catalyst for oxidative dehydrogenation of ethane. *Journal of the Iranian Chemical Society*, 16(2), 299-310. https://doi.org/10.1007/s13738-018-1510-4.

Ali, S., Zahid, A., & Shahid, S. T. (2023): Green engineering of iron and iron oxides by different plant extract. In *Iron Ores and Iron Oxides-New Perspectives*. IntechOpen. DOI: 10.5772/intechopen.1001910

Al-Musawi, T. J., Mahvi, A. H., Khatibi, A. D., & Balarak, D. (2021): Effective adsorption of ciprofloxacin antibiotic using powdered activated carbon magnetized by iron (III) oxide magnetic nanoparticles. *Journal of porous materials*, *28*, 835-852.

Aryal, S., Baniya, M. K., Danekhu, K., Kunwar, P., Gurung, R., and Koirala, N. (2019): Total phenolic content, flavonoid content and antioxidant potential of wild vegetables from Western Nepal. *Plants*, 8(4), 96.

Aswathi, V. P., Meera, S., Maria, C. A., & Nidhin, M. (2023): Green synthesis of nanoparticles from biodegradable waste extracts and their applications: a critical review. *Nanotechnology for Environmental Engineering*, *8*(2), 377-397.

Azizi, A. (2021): Green synthesis of iron oxide/cellulose magnetic recyclable nanocomposite and its evaluation in ciprofloxacin removal from aqueous solutions. *Journal of the Iranian Chemical Society*, *18*(2), 331-341.

Ayawei, N., Ebelegi, A. N., & Wankasi, D. (2017). Modelling and Interpretation of Adsorption Isotherms. *Journal of Chemistry*, 2017, Article ID 3039817. https://doi.org/10.1155/2017/3039817.

Bakatula, E. N., Richard, D., Neculita, C. M., and Zagury, G. J. (2018): Determination of point of zero charge of natural organic materials. *Environmental Science and Pollution Research*, 25, 7823-7833.

Balamurugan, M., Saravanan, S., and Soga, T. (2014): Synthesis of iron oxide nanoparticles by using Eucalyptus globulus plant extract. *E-Journal of Surface Science and Nanotechnology*, 12, 363-367.

Bashir, M., Ali, S., & Farrukh, M. A. (2020): Green synthesis of Fe_2O_3 nanoparticles from orange peel extract and a study of its antibacterial activity. *Journal of the Korean Physical Society*, 76, 848-854.

Chaudhari, D. S., Upadhyay, R. P., Shinde, G. Y., Gawande, M. B., Filip, J., Varma, R. S., & Zboril, R. (2024): A review on sustainable iron oxide nanoparticles: synthesis and application in organic catalysis and environmental remediation. *Green Chemistry*. **26,** 7579-7655

Cheng, W., Zhang, W., Hu, L., Ding, W., Wu, F., & Li, J. (2016). Etching synthesis of iron oxide nanoparticles for adsorption of arsenic from water. *Rsc Advances*, 6(19), 15900-15910.

de Oliveira Carvalho, C., Costa Rodrigues, D. L., Lima, É. C., Santanna Umpierres, C., Caicedo Chaguezac, D. F., & Machado Machado, F. (2019): Kinetic, equilibrium, and thermodynamic studies on the adsorption of ciprofloxacin by activated carbon produced from Jerivá (Syagrus romanzoffiana). *Environmental Science and Pollution Research*, 26, 4690-4702.

Demirezen, D. A., Yıldız, Y. Ş., Yılmaz, Ş., & Yılmaz, D. D. (2019): Green synthesis and characterization of iron oxide nanoparticles using Ficus carica (common fig) dried fruit extract. *Journal of bioscience and bioengineering*, 127(2), 241-245.

Dhal, J. P., Dash, T., & Hota, G. (2020). Iron oxide impregnated mesoporous MCM-41: synthesis, characterization and adsorption studies. *Journal of Porous Materials*, 27, 205-216.

Eapen JV, Thomas S, Antony S, George P, Antony J. (2024): A review of the effects of pharmaceutical pollutants on humans and aquatic ecosystem. *Explor Drug Sci*, 2:484–507. https://doi.org/10.37349/eds.2024.00058

Elkhateeb, O., Atta, M. B., & Mahmoud, E. (2024): Biosynthesis of iron oxide nanoparticles using plant extracts and evaluation of their antibacterial activity. *AMB Express*, *14*(1), 92.

Faisal, S., Jan, H., Shah, S. A., Shah, S., Khan, A., Akbar, M. T., Rizwan, M., Jan, F., Wajidullah, and Akhtar, N. (2021): Green synthesis of zinc oxide (ZnO) nanoparticles using aqueous fruit extracts of Myristica fragrans: their characterizations and biological and environmental applications. *ACS Omega*, 6(14), 9709–9722.

Gor, A. H., & Dave, P. N. (2020): Adsorptive abatement of ciprofloxacin using $NiFe_2O_4$ nanoparticles incorporated into G. ghatti-cl-P (AAm) nanocomposites hydrogel: isotherm, kinetic, and thermodynamic studies. *Polymer Bulletin*, *77*(11), 5589-5613.

Hernández-Hernández, A. A., Aguirre-Álvarez, G., Cariño-Cortés, R., Mendoza-Huizar, L. H., & Jiménez-Alvarado, R. (2020): Iron oxide nanoparticles: synthesis, functionalization, and applications in diagnosis and treatment of cancer. *Chemical Papers*, *74*(11), 3809-3824.

Hussain, M., Hussaini, S. S., Shariq, M., Alzahrani, H., Alholaisi, A. A., Alharbi, S. H., ... & Seku, K. (2023): Enhancing Cu^{2+} Ion removal: an innovative approach utilizing modified frankincense gum combined with multiwalled carbon tubes and iron oxide nanoparticles as adsorbent. *Molecules*, *28*(11), 4494.

Ibraheem, D. R., Hussein, N. N., Sulaiman, G. M., Mohammed, H. A., Khan, R. A., & Al Rugaie, O. (2022): Ciprofloxacin-loaded silver nanoparticles as potent nano-antibiotics against resistant pathogenic bacteria. *Nanomaterials*, *12*(16), 2808.

Jamzad, M., and Kamari Bidkorpeh, M. (2020): Green synthesis of iron oxide nanoparticles by the aqueous extract of Laurus nobilis L. leaves and evaluation of the antimicrobial activity. *Journal of Nanostructure in Chemistry*, 10(3), 193–201.

Khan, A. H. A., & Barros, R. (2023): Pharmaceuticals in water: risks to aquatic life and remediation strategies. *Hydrobiology*, *2*(2), 395-409.

Khasevani, S. G., Nikjoo, D., Chaxel, C., Umeki, K., Sarmad, S., Mikkola, J. P., & Concina, I. (2023): Empowering Adsorption and Photocatalytic Degradation of Ciprofloxacin on BiOI Composites: A Material-by-Design Investigation. *ACS omega*, *8*(46), 44044-44056.

Lavín Flores, A., Medina-Berríos, N., Pantoja-Romero, W., Berríos Plaza, D., Kisslinger, K., Beltran-Huarac, J., ... & Weiner, B. R. (2024): Geometry and Surface Area Optimization in Iron Oxide Nanoparticles for Enhanced Magnetic Properties. *ACS omega*, *9*(30), 32980-32990.

López-Luna, J., Ramírez-Montes, L. E., Martinez-Vargas, S., Martínez, A. I., Mijangos-Ricardez, O. F., González-Chávez, M. D. C. A., ... & Vázquez-Hipólito, V. (2019): Linear and nonlinear kinetic and isotherm adsorption models for arsenic removal by manganese ferrite nanoparticles. *SN Applied Sciences*, *1*, 1-19.

Mehta, J., Dhaka, R. K., Dilbaghi, N., Lim, D. K., Hassan, A. A., Kim, K. H., and Kumar, S. (2022): Recent advancements in adsorptive removal of organophosphate pesticides from aqueous phase using nanomaterials. *Journal of Nanostructure in Chemistry*, 1-18.

Mutia, A. S., Ariyanto, T., and Prasetyo, I. (2022): Ciprofloxacin removal from simulated wastewater through a combined process of adsorption and oxidation processes using Fe/C adsorbent. *Water, Air, and Soil Pollution*, 233(4), 146.

Naqvi, S. A. Z., Irfan, A., Zaheer, S., Sultan, A., Shajahan, S., Rubab, S. L., ... & Acevedo, R. (2021). Proximate composition of orange peel, pea peel and rice husk wastes and their potential use as antimicrobial agents and antioxidants. *Vegetos*, *34*, 470-476.

Ogbezode, J. E., Ezealigo, U. S., Bello, A., Anye, V. C., & Onwualu, A. P. (2023): A narrative review of the synthesis, characterization, and applications of iron oxide nanoparticles. *Discover Nano*, *18*(1), 125.

Oliveira, M. G., Rocca, D. G. D., Moreira, R. D. F. P. M., da Silva, M. G. C., & Vieira, M. G. A. (2024): Enhanced degradation and removal of ciprofloxacin and ofloxacin through advanced oxidation and adsorption processes using environmentally friendly modified carbon nanotubes. *Environmental Science and Pollution Research*, *31*(20), 29957-29970.

Ortúzar, M., Esterhuizen, M., Olicón-Hernández, D. R., González-López, J., & Aranda, E. (2022): Pharmaceutical pollution in aquatic environments: a concise review of environmental impacts and bioremediation systems. *Frontiers in microbiology*, *13*, 869332.

Papaioannou, C., Geladakis, G., Kommata, V., Batargias, C., & Lagoumintzis, G. (2023): Insights in Pharmaceutical Pollution: The Prospective Role of eDNA Metabarcoding. *Toxics*, *11*(11), 903.

Priya, Naveen, Kaur, K., and Sidhu, A. K. (2021): Green synthesis: An eco-friendly route for the synthesis of iron oxide nanoparticles. *Frontiers in Nanotechnology*, *3*, 655062.

Razack, S. A., Suresh, A., Sriram, S., Ramakrishnan, G., Sadanandham, S., Veerasamy, M., ... and Sahadevan, R. (2020): Green synthesis of iron oxide nanoparticles using Hibiscus rosa-sinensis for fortifying wheat biscuits. *SN Applied Sciences*, *2*, 1-9.

Rojo, C., Carmona, E. R., Hernández-Saravia, L. P., Villacorta, A., Marcos, R., Carevic, F. S., ... & Nelson, R. (2024): Utilization of Orange Peel Waste for the Green Synthesis of Iron Nanoparticles and its Application to Stimulate Growth and Biofortification on Solanum lycopersicum. *Waste and Biomass Valorization*, 1-14.

Sassa-Deepaeng, T., Khumpirapang, N., Yodthong, W., Myat, Y. Y., Anuchapreeda, S., & Okonogi, S. (2024): Effects of Salts and Other Contaminants on Ciprofloxacin Removal Efficiency of Green Synthesized Copper Nanoparticles. *Veterinary Sciences*, *11*(4), 179.

Savari, M. N., & Jabali, A. (2023): Properties of Iron Oxide Nanoparticles (IONPs). In *Theranostic Iron-Oxide Based Nanoplatforms in Oncology: Synthesis, Metabolism, and Toxicity for Simultaneous Imaging and Therapy* (pp. 49-65). Singapore: Springer Nature Singapore.

Shah, S. W. A., Rehman, M. U., Hayat, A., Tahseen, R., Bajwa, S., Islam, E., ... & Niazi, N. K. (2022): Enhanced degradation of ciprofloxacin in floating treatment wetlands augmented with bacterial cells Immobilized on Iron oxide Nanoparticles. *Sustainability*, *14*(22), 14997.

Shah, S. W. A., Rehman, M. U., Hayat, A., Tahseen, R., Bajwa, S., Islam, E., ... & Niazi, N. K. (2022). Enhanced degradation of ciprofloxacin in floating treatment wetlands augmented with bacterial cells Immobilized on Iron oxide Nanoparticles. *Sustainability*, *14*(22), 14997.

Singh, S., & Goswami, N. (2021): Structural, optical, magnetic and dielectric properties of magnetite (Fe 3 O 4) nanoparticles prepared by exploding wire technique. *Journal of Materials Science: Materials in Electronics*, *32*, 26857-26870.

Sithara, N. V., Bharathi, D., Lee, J., Mythili, R., Devanesan, S., & AlSalhi, M. S. (2024): Synthesis of iron oxide nanoparticles using orange fruit peel extract for efficient remediation of dye pollutant in wastewater. *Environmental Geochemistry and Health*, *46*(2), 30.

Stan, M., Lung, I., Soran, M. L., Leostean, C., Popa, A., Stefan, M., ... and Porav, A. S. (2017): Removal of antibiotics from aqueous solutions by green synthesized magnetite nanoparticles with selected agro-waste extracts. *Process Safety and Environmental Protection*, *107*, 357-372.

Thi, T. U. D., Nguyen, T. T., Thi, Y. D., Thi, K. H. T., Phan, B. T., & Pham, K. N. (2020). Green synthesis of ZnO nanoparticles using orange fruit peel extract for antibacterial activities. *RSC advances*, *10*(40), 23899-23907.

Varghese, L., Veena Gopalan, E., & Rymond, A. (2023): Synthesis and characterisation of iron oxide nanoparticles using leaf extract of Ficus religiosa. In *AIP Conference Proceedings* (Vol. 2783, No. 1). AIP Publishing.

Vikram, S., Vasanthakumari, R., Tsuzuki, T., & Rangarajan, M. (2016): Investigations of suspension stability of iron oxide nanoparticles using time-resolved UV–visible spectroscopy. *Journal of Nanoparticle Research*, *18*, 1-24.

Vijaykumar, A., Bolhuis, P. G., & Ten Wolde, P. R. (2016). The intrinsic rate constants in diffusion-influenced reactions. *Faraday Discussions*, *195*, 421-441

Xing, X., Feng, J., Lv, G., Song, K., Mei, L., Liao, L., ... & Xu, B. (2015). Adsorption mechanism of ciprofloxacin from water by synthesized birnessite. *Advances in Materials Science and Engineering*, *2015*(1), 148423.

Yassin, M. T., Al-Otibi, F. O., Al-Askar, A. A., & Alharbi, R. I. (2023): Green synthesis, characterization, and antifungal efficiency of biogenic iron oxide nanoparticles. *Applied Sciences*, *13*(17), 9942.